Microdisk lasers based on InGaAs/GaAs quantum dots monolithically integrated with a waveguide

© N.A. Fominykh[1], N.V. Kryzhanovskaya[1], S.D. Komarov[1], I.S. Makhov[1], K.A. Ivanov[1], E.I. Moiseev[1], E.E. Antonov[1], Yu.A. Guseva[2], M.M. Kulagina[2], S.A. Mintairov[2], N.A. Kalyuzhnyy[2], R.A. Khabibullin[3], R.R. Galiev[3], A.Yu. Pavlov[3], K.N. Tomosh[3], A.E. Zhukov[1]

[1] National Research University „Higher School of Economics“,
190008 St. Petersburg, Russia
[2] Ioffe Institute,
194021 St. Petersburg, Russia
[3] Institute of Ultra High Frequency Semiconductor Electronics of RAS,
117105 Moscow, Russia

E-mail: fominy-nikita@yandex.ru

Received February 10, 2024
Revised March 18, 2024
Accepted April 5, 2024

Microdisk lasers with diameters of 30 and 40 μm with an active region based on InGaAs/GaAs quantum dots, laterally coupled to an optical waveguide, were studied. The microlasers and waveguides were fabricated in a single process on a single GaAs substrate. The spectral characteristics at elevated injection currents on the microlaser and/or waveguide exceeding the lasing threshold by up to 4 times were investigated. The possibility of reducing absorption losses in the waveguide by applying a direct bias to it was shown. An optocouple in which a microdisk laser coupled to a waveguide serves as a radiation source and a waveguide photodetector as a radiation receiver was realized. The dark current density of the waveguide photodetector was 1.1 μA/cm^2 at a reverse bias of -6 V.

Keywords: Microlasers, quantum dots, waveguides, optocouple, waveguide photodetector.

DOI: 10.61011/SC.2024.02.58365.6049

1. Introduction

Photonic integrated circuits (PIC) have a higher data transfer rate and lower power consumption, compared with electronic circuits [1]. The implementation of PIC on GaAs represents a promising alternative to PIC on Si, since both materials have, unlike Si, GaAs is a straight-band semiconductor [2]. Semiconductor microlasers with a disk-shaped resonator supporting whispering gallery modes (WGM) [3] can be used as radiation sources in PIC. Microdisc (MD) lasers have high Q-factor, and their radiation propagates in the plane of the substrate [4]. A directional radiation output is required for the successful implementation of PIC based on such microlasers, which is hindered by the circular symmetry of the MD resonator [5]. One of the most promising solutions to this problem is the optical coupling of MD lasers with an optical waveguide (OW) [6]. The implementation of this type of coupling can be performed in a vertical [7,8] or a lateral configuration [9]. Due to its compactness and stability, the monolithic integration of the MD laser and OW is of the greatest interest. In this case, both elements are formed from the same epitaxial structure. This has previously been demonstrated for AlGaInAs/InP microlasers [10]. Compared with InP materials, GaAs materials are characterized by higher energy zone discontinuities and jumps in the refractive index, as well as higher thermal conductivity.

The possibility of monolithic integration of a MD laser and OW created on the basis of a heterostructure with quantum dots (QD) on a GaAs substrate was shown for the first time in Ref. [11]. Radiation absorption losses caused by „interband“ transitions in the QD of the active region of OW made of the same epitaxial structure as MD lasers limited the output power. We studied the possibility of reducing the absorption losses in OW in this paper when a forward bias is applied to it. The active region based on InGaAs/GaAs quantum dots is characterized by a low level of pumping necessary for bleaching, which reduces the heating of the structure. Another advantage of QD is the extremely small (μA/cm^2) dark currents when used as the active region of the photodetector (PD) [12,13]. Radiation absorption in waveguide PD takes place along the entire length of the strip, which is especially important for nanostructures characterized by a relatively low level of absorption. Thus, waveguide PD based on QD can, together with MD lasers with a QD active region, form an optocoupler with a consistent operating wavelength, which can be used, for example, as a compact micro sensor [14]. We have considered the possibility of implementing an optocoupler consisting of an InGaAs/GaAs QD-based MD laser with an active region, monolithically coupled with OW, and a waveguide PD formed from a similar heterostructure with QD.

2. Experiment

The heterostructure was synthesized by gas-phase epitaxy from organometallic compounds on a substrate n^+-GaAs,

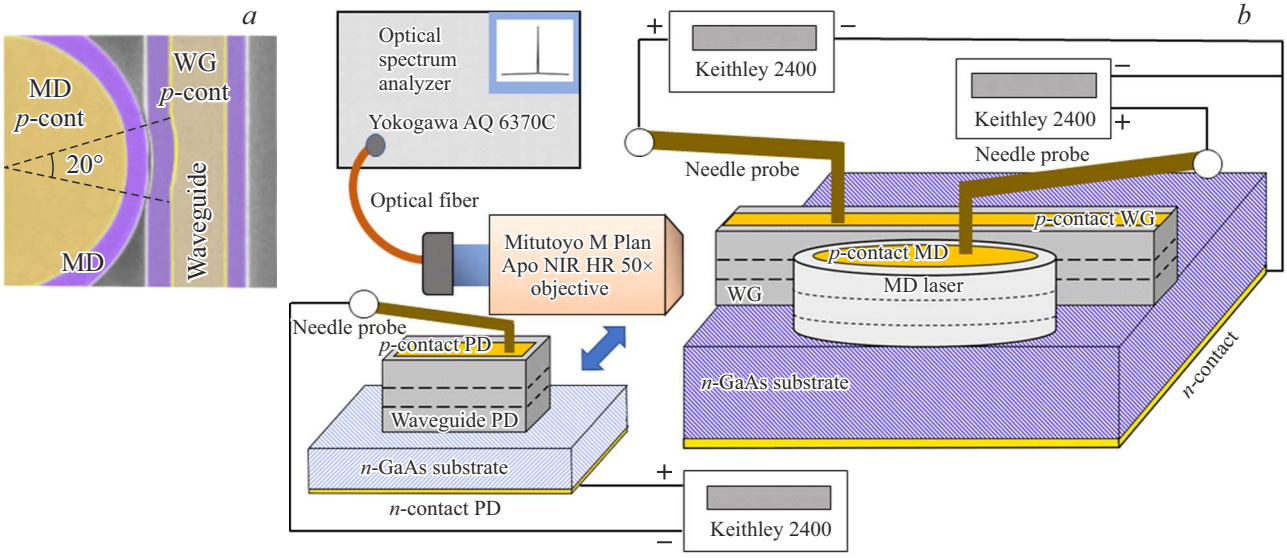

Figure 1. *a* — 30 μm MD laser coupled with an envelope section corresponding to an angle of 20°, *b* — experimental setup and optocoupler. (The colored version of the figure is available on-line).

oriented at 6° relative to the plane (100). The structure consisted of a buffer layer n^+-GaAs, a lower emitter layer *n*-AlGaAs 1.5 mm thick with a doping level $\sim 7 \cdot 10^{17}$ cm^{-3}, 0.75 μm of the unalloyed GaAs waveguide layer, 1.5 μm of the upper emitter layer *p*-AlGaAs ($7 \cdot 10^{17}$ cm^{-3}) and the contact layer p^{++}-GaAs 0.35 mm thick. The molar fraction of AlAs in AlGaAs layers was 39%. The active region consisting of 5 InGaAs/GaAs QD layers was located in the waveguide layer. The QD were formed by deposition of a 2 nm thick layer of $In_{0.4}Ga_{0.6}As$, the QD layers were separated by a 40 nm thick GaAs spacer. The mechanism of QD formation with this deposition method is discussed in Ref. [15].

The technology of a semiconductor inductively coupled plasma-reactive ion etching (ICP-RIE Sentech SI500, BCl_3/Ar) was used to form MD lasers and OW. The multilayer system of dielectrics $Si_3N_4/SiO_2/Al_2O_3$ developed at the Higher School of Economics of the Russian Academy of Sciences was used as a rigid mask, the figure in which is also anisotropically etched using a multistage process, first in chlorine plasma, then in fluorinated plasma. A pattern in a negative electron resistor ma-N2403 (Microresist Technology GmbH) formed by electron beam lithography (Raith Voyager, 50 kV) was used as the primary mask. This resulted in a large etching depth of the mesa with a vertical wall and a small gap between the microlaser and the OW. The etching depth during the formation of both MD and OW was equal to 4 μm, i. e., the heterostructure was etched through. The chosen OW width was 10 μm, and its length was 440 μm. The MD diameter was equal to 30 and 40 μm. The distance between the microlasers and the OW was 100 nm. The output power from the end of OW is limited by the low efficiency of optical coupling as noted in Ref. [10]. The OW enveloped the MD laser along the arc corresponding to the angle 20° to increase the efficiency of optical coupling [10,16] (Figure 1, *a*). *P*-contacts were formed by applying AgMn/Ni/Au metallization to the contact layer of p^{++}-GaAs. The contacts on OW were made in the form of a strip with a width of 8 μm, and they had the shape of circles of different diameters (28 or 38 μm) on MD lasers. The GaAs substrate was thinned and AuGe/Ni/Au *n*-contact was applied to its back side.

A heterostructure similar to the laser one was used to create the PD, but 6 InGaAs/GaAs QD layers were placed in the GaAs waveguide layer. Strip-shaped PD with a width of 50 μm and a length of the absorbing region of 92 μm were produced by photolithography and dry etching (STE ICPe68). The height of the PD mesa was ~ 5.5 μm. The ohmic contacts were formed using MD laser technology. The light-absorbing facets of PD structures were formed by splitting PD crystals without applying additional antireflective coatings.

All electroluminescence (EL) studies covered in this paper were performed at room temperature, and the structures were continuously powered. A needle probe made of tungsten with a diameter of 15 mm was used for the contact to the upper electrode of the studied structures. The sample was placed with the *n*-contact down on a copper holder. The electrical circuit for applying the forward bias to the OW and the electrical circuit for pumping the MD laser had a common negative contact. Keithley 2400 meter source was used as a current source. The radiation was collected using Mitutoyo M Plan Apo NIR HR 50x micro lens when it was focused on the studied MD laser or on the end of the laser associated with it. The EL spectrum was recorded using Yokogawa AQ 6370C optical spectrum analyzer with a spectral resolution of 0.2 nm. The radiation collected by the micro lens was transmitted through an optical fiber to

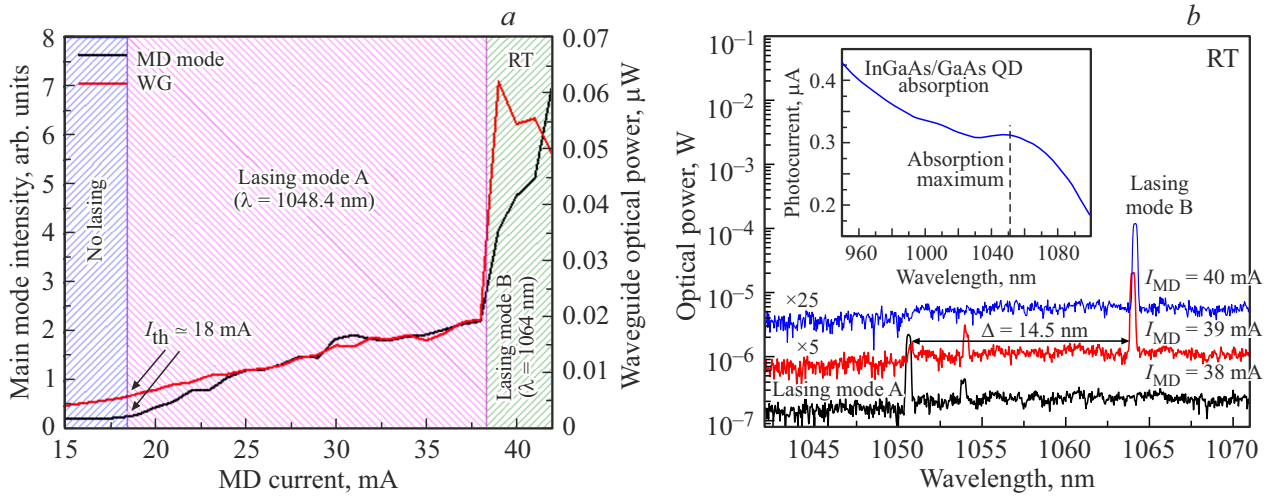

Figure 2. *a* — dependences of the optical output power from the end of OW and intensity of the main laser mode on the pumping current of the MD laser with a diameter of 30 μm. *b* — the EL spectra of 30 μm MD laser. The spectra are shifted along the ordinate axis to facilitate perception. The inset shows the dependence of the photocurrent on the wavelength for PD with a light-absorbing region on InGaAs/GaAs QD [13].

the photodiode sensor of Thorlabs PM100D optical power meter for measuring the optical power. In case of collection of radiation from the MD laser, we assume that only about 30% of the total optical power falls on the photodiode sensor due to the azimuthal isotropy of the radiation of the microlaser [17]. The EL setup diagram is shown in Figure 1, *b*.

The laser coupled with the OW and the PD were on different chips for the implementation of the MD optocoupler. Micrometric movements were used to accurately position the waveguide PD relative to the end face of OW. The reverse bias was applied to the PD and the photocurrent was measured using Keithley 2400 measuring source in accordance with the diagram shown in Figure 1, *b*

3. Experimental results

Initially, the intensity as well as the emission spectra of the microlaser from the end of the OW were studied without applying a bias to the OW. Figure 2, *a* shows the dependence of the integral intensity of the main (brightest) laser mode on the injection current of the MD laser. The threshold current (I_{th}) was determined by the inflection of this dependence and for an MD laser with a diameter of 30 μm was 18 mA. A sharp increase of the intensity of the main laser mode is observed at a pump current of $\sim$ 39 mA, amounting to $\sim 2I_{th}$. Figure 2, *a* also shows the dependence of the output optical power from the end of the OW, which, as can be seen, generally repeats the course of the dependence of the intensity of the main mode. The study of the EL spectra of the MD laser (Figure 2, *b*) showed that the laser mode A is dominant in the EL spectrum with a pump current from I_{th} to 38 mA. The spectral position of this mode with an injection current equal to the threshold value corresponds to 1048.4 nm, and it corresponds to 1050.5 nm when the pumping current increases to 38 mA. The laser generation is switched from the wavelength $\sim$ 1050.5 nm to $\sim$ 1064 nm with the injection current of $\sim 2I_{th}$ (39–40 mA) (laser mode B). This switching is attributable to the self-heating of the laser and the shift of the gain spectrum to the long-wavelength region. The spectral distance between these modes (14.5 nm) is significantly greater than the inter-mode interval ($FSR \simeq 3.3$nm) for an WGM MD laser with a diameter of 30 μm. Such a strong change in the wavelength of laser generation, therefore, cannot be explained by a jump in generation to an adjacent, longer-wavelength WGM because of heating of the microlaser with an increase of the current, which is often observed in MD lasers not coupled to a waveguide.

We believe that this behavior can be associated with additional losses caused by the absorption of microlaser radiation in the OW. The highest losses will be introduced near the maximum absorption of InGaAs/GaAs QD in the WGM. The absorption maximum in InGaAs/GaAs QD corresponds to the wavelength of $\lambda \simeq 1052$ nm (see insert to Figure 2, *b*). The maximum gain spectrum of the pumped active region is approximately in the same spectral range since the laser is also generated near this wavelength ($\sim$ 1048.4 nm). Thus, the laser mode is strongly absorbed by the waveguide near the generation threshold. The gain developed by the active region of the MD laser near the generation threshold is not sufficient to overcome optical losses in case of longer waves, even taking into account the fact that absorption in OW is lower for them. However, the laser is generated at a wavelength of $\sim$ 1064 nm (mode B) when the pumping current becomes large enough, and a shorter wavelength mode A goes out. This indicates the fact that there is no pinning of the Fermi level in the active

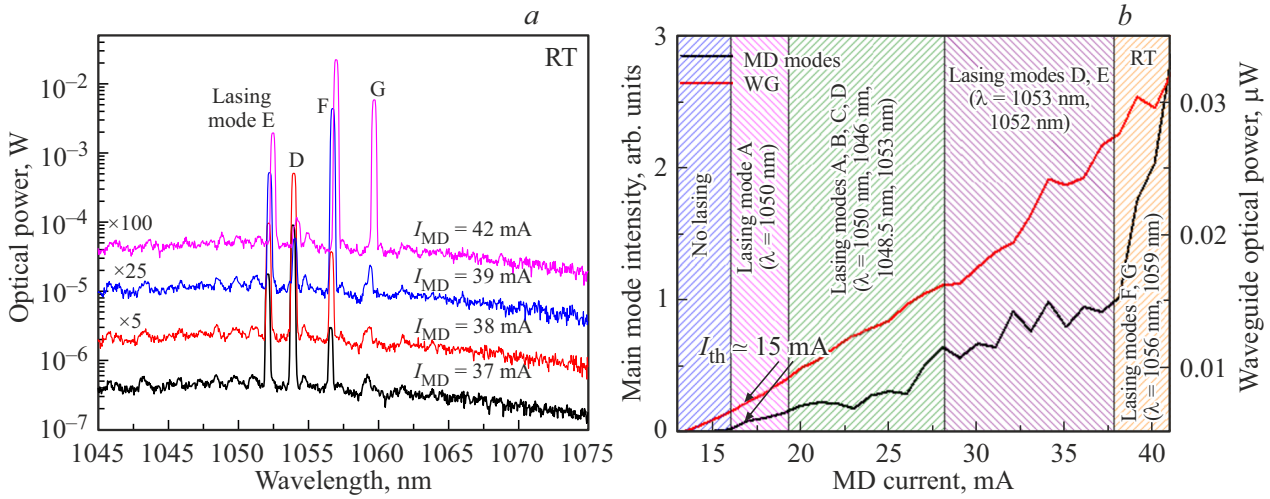

Figure 3. *a* — EL spectra of 40 μm MD laser. The spectra are shifted along the ordinate axis to facilitate perception. *b* — dependences of the optical output power from the end of OW and intensity of the main laser mode on the pumping current of the MD laser with a diameter of 40 μm.

region of the MD laser, when the generation threshold is reached, but the concentration of charge carriers continues to increase. This in turn causes a gradual increase of the gain of the long-wavelength region. When the pumping current changes from 38 to 39 mA, the laser mode B is formed at the wavelength of $\sim$ 1064 nm, which has almost 3 times the intensity than the shorter-wave mode A. As already mentioned, the output power from the end of OW also steeply grows (Figure 2, *a*). It should be noted that the jump of the generation wavelength indicates that the sharp increase of power is not associated with the bleaching of the waveguide by radiation emitted from the microdisc. In this case, there is no reason for a wavelength jump.

The EL spectra of the studied MD laser with a diameter of 40 μm, which were obtained with a zero forward bias on OW, are shown in Figure 3, *a*. A large number of laser modes are present in the EL spectrum for microlasers of this diameter. This fact can be attributed to the lower efficiency of radiation output in OW from this higher quality microresonator. In particular, this is manifested in the lower threshold current (15 mA) of the studied 40 μm MD lasers compared to 30 μm (18 mA).

Microlasers also demonstrate laser generation in the spectral region close to the maximum absorption of QD near the generation threshold of 40 μm. The analysis of the dependence of the optical power on the pumping current demonstrates, as in the case of 30 μm microlasers, a noticeable increase of the intensity of the MD laser radiation from the end of OW starting from a certain injection current above the generation threshold. An abrupt change of the intensity of the main laser mode is also observed at the same time. The current corresponding to these effects was $\sim$ 37 mA for microlazers with a diameter of 40 μm (Figure 3, *b*). Similarly to 30 μm MD lasers, there are steep changes of the intensity of the main laser mode and the values of the optical power from the end of OW are associated with the appearance of long-wave modes at 1056 and 1059 nm wavelengths (modes F and G). At the same time, however, an increase of the output optical power from the end of OW is not as significant as in the case of 30 μm MD lasers. This is probably due to the higher Q-factor of 40 μm MD lasers and therefore a smaller contribution to the total losses made by the output of the radiation in OW.

The application of a forward bias to the OW can reduce absorption in it due to the injection of nonequilibrium charge carriers. Thus, the absorption in the OW will decrease with an increase of the forward bias until the active region is completely bleached. However, the forward bias also results in the appearance of a spontaneous EL of the OW. At the same time, the intensity of this effect will increase in proportion to the magnitude of the current through the OW. In addition, laser generation may occur in the case of sufficiently high pumping currents.

Thus, the EL spectra of the MD laser obtained from the end of the OW when a forward bias is applied to it will also contain the OW radiation. To correctly assess the effect of the bleaching of the active area of the OW it is desirable to exclude its contribution from the obtained results. To do this, we measured the spectra of the electron with different forward bias on it, whereas the pumping current of the MD laser was zero (Figure 4). The OW laser is generated when the forward bias current reaches the value of $\sim$ 60 mA. This effect results in the fact that the radiation from OW overlaps the radiation of the microlaser and the structure heats up strongly and the thermal rollover of the optical power of the MD laser occurs at lower values of the pumping current. The current on the OW did not exceed 35 mA during subsequent measurements.

Figure 5 shows the dependences of the optical power of MD lasers obtained from the end of the laser on the

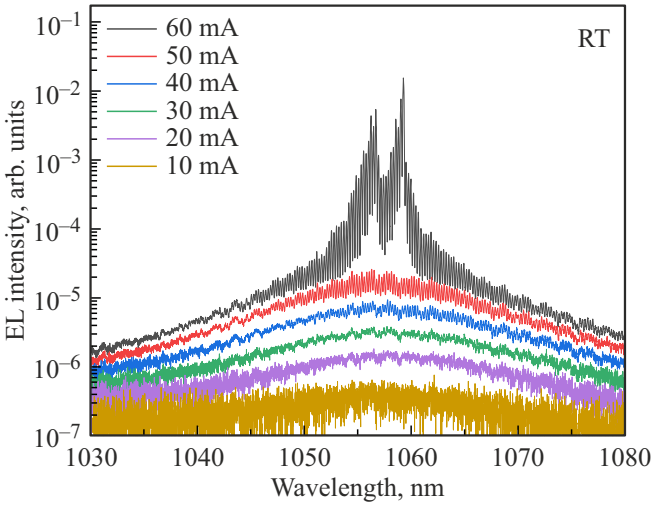

Figure 4. Typical EL spectra with different forward bias on the studied OW.

pumping current of the laser and with various currents on the OW (from 0 to 35 mA). The optical power entering the detector consisted only of the radiation of the OW itself with a zero current through the MD laser and a non-zero forward bias on the OW. We set the value of the optical power obtained in the absence of current on the MD laser as 0 to exclude its contribution. As can be seen from Figure 5, the application of a forward bias on the OW results in a significant increase of the optical power output from its end of the MD laser itself, both for 30 μm and 40 μm microlasers. The largest value of the forward bias current on the OW 35 mA used in the study results in an increase of the output optical power of the MD laser by almost an order of magnitude over the entire range of MD laser pumping currents above the threshold value. At the same time, the threshold current of MD lasers did not change in the entire studied current range (within the limits of ± 0.5 mA).

There is a sharp inflection (intensity jump), similar to the one discussed above for the case of OW without pumping on the dependencies shown in Figure 5. In this case, the current on the MD laser (I_{bend}) corresponding to this bend decreases with an increase of the forward bias on OW. For example, the value of the current at which the jump occurs decreases from 39 to 33 mA for an MD laser with a diameter of 30 μm. As noted above, a sharp increase of optical power occurs when longer-wavelength modes appear in the microlaser EL spectrum. Thus, the bleaching of the active region of OW caused by the application of a forward bias to it results in an increase of the Q-factor (loss reduction) of the long-wave modes of the MD laser and, accordingly, their appearance in the spectrum at lower values of the injection current through the microlaser.

Next, we implemented and studied an optocoupler, which is an MD laser coupled with OW and a waveguide PD. The diameter of the microlaser used was 30 μm. The length of the waveguide PD was 92 μm, and the width was ~ 50 μm. The dark current of the PD has a significant effect on its characteristics, therefore, the dependence of this characteristic on the magnitude of the reverse bias on the PD was obtained (Figure 6, *a*). The values of the dark current did not exceed 1.2 nA (26 μA/cm^2) with the reverse bias of ~ 20 V. The dark current was ~ 40 pA with the bias of ~ 6 V which corresponds to the current density of ~ 0.9 μA/cm^2. For comparison, a dark current density of 0.35 μA/cm^2 was reported in Ref. [18] for photodetectors based on InAs/InGaAs quantum dots, but the reverse voltage was only -1 V. As can be seen from Figure 6, *a*,

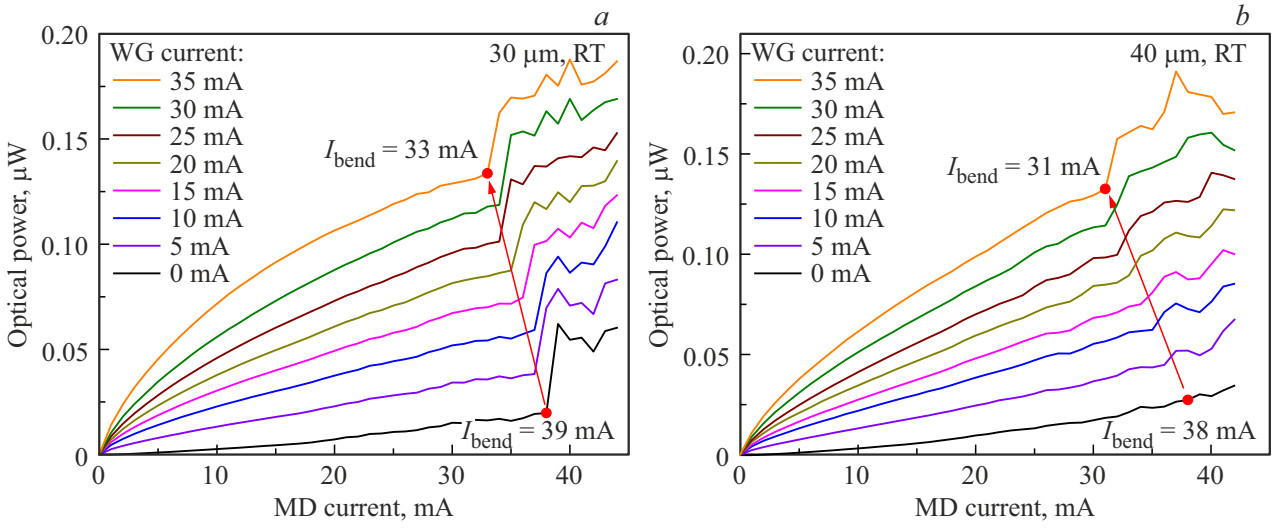

Figure 5. The dependence of the optical power output from the end of the OW on the pumping current of the MD laser, with different forward bias currents on the OW for 30 μm (*a*) and 40 μm (*b*) MD lasers. The red arrows shows the change of the magnitude of the current (I_{bend}), at which the laser mode jumps to a longer wavelength, with an increase of the current through OW. (The colored version of the figure is available on-line).

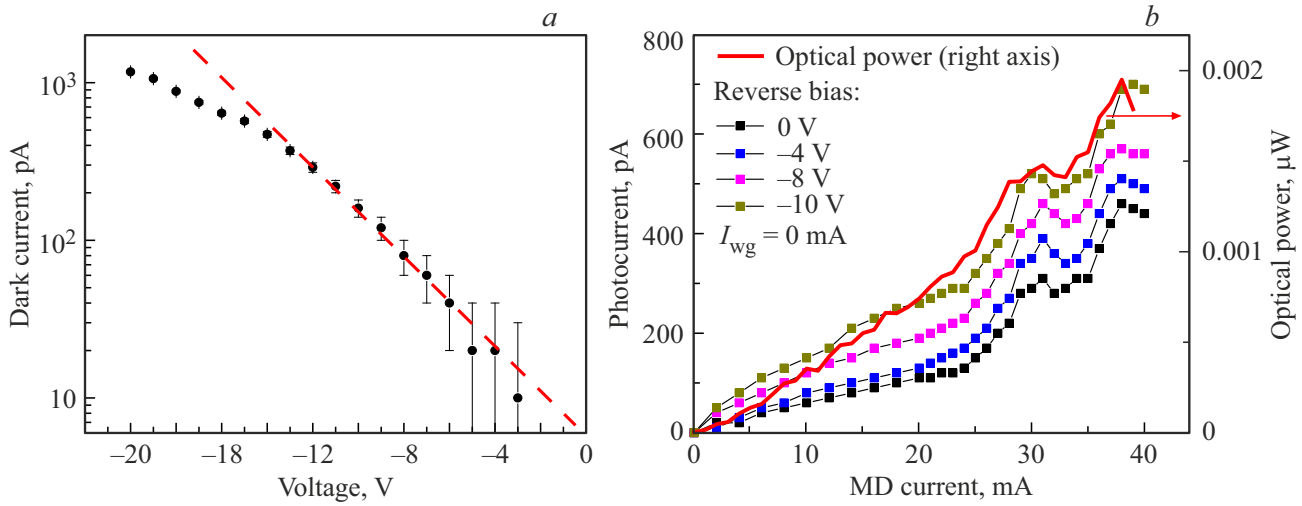

Figure 6. *a* — dependence of the magnitude of the dark current of the PD on the reverse bias. The red dotted line indicates a linear approximation of the measurement results with a small reverse offset. *b* — dependences of the magnitude of the photocurrent PD on the current on the MD laser at different reverse displacement (left axis) and the dependence of the optical power of the MD laser output from the end of the OW on the pumping current (right axis).

the magnitude of the dark currents with the reverse bias of less than -6 V is within the error range of the device used. However, it should be noted that extrapolation of the measured results (the red dotted line in Figure 6, *a*) to the area of -2 V provides the value of ~ 10 pA ($0.21\,\mu$A/cm^2). Such small dark currents of the studied PD indicate the high structural perfection of its heterostructure and the small size of surface leaks.

The waveguide PD was parallel to the OW when implementing the optocoupler, the distance between their ends was 260 μm. The active region of the PD was at the same altitude level with the active region of the OW to ensure maximum efficiency of radiation capture. Figure 6, *b* shows the dependences of the photocurrent on the injection current of the MD laser, which were obtained at different values of the reverse bias on the PD (from 0 to -10 V). The magnitude of the photocurrent at zero pumping of the MD laser was reduced to 0 by subtracting the dark current of the PD for each of the obtained dependences. An increase of the reverse bias on the PD results in an increase of photocurrent due to a stronger curvature of the $p-n$-transition. The dependence of the optical power of the MD laser output from the end of the OW on the injection current of the MD laser is also shown in Figure 6, *b* (right axis). The identical nature of the dependence of the photocurrent and the dependence of the optical power indicate the detection of PD of the MD laser radiation, i. e., the successful implementation of the optocoupler.

4. Conclusion

The spectral characteristics with the injection current $\sim 2I_{th}$ of MD lasers of different diameters with an active region based on InGaAs/GaAs QD laterally coupled to OW with an envelope section of 20° were studied in this paper. An almost threefold increase of output power from the OW was demonstrated when a laser line appears in the spectra of EL microlasers in the long-wavelength part of the spectrum. The application of a forward bias to the OW results in a partial bleaching of its active region and an increase of the output optical power from its end face. At the same time, the bleaching of the active area of the OW increases the Q-factor of the long-wave modes of the MD laser, which causes their earlier appearance in the EL spectrum. An optocoupler is implemented with a radiation source in the form of an MD laser coupled with an OW, and with a receiver in the form of a waveguide FD.

Acknowledgments

The work was carried out on the equipment of the large-scale research facilities „Complex optoelectronic stand of the National Research University Higher School of Economics — Saint-Petersburg“.

Funding

This study was supported by grant No. 22-72-10002 from the Russian Science Foundation, https://rscf.ru/project/22-72-10002/. The study of the optocoupler was carried out as part of the Fundamental Research Program of the National Research University Higher School of Economics.

Conflict of interest

The authors declare that they have no conflict of interest.

References

[1] X. Mu, S. Wu, L. Cheng, H.Y. Fu. Appl. Sci., **10** (4), 1538 (2020).
[2] P. Jiang and K.C. Balram. Opt. Express, **28** (8), 12262 (2020).
[3] N. Kryzhanovskaya, A. Zhukov, E. Moiseev, M. Maximov. J. Phys. D: Appl. Phys., **54** (45), 453001 (2021).
[4] F. Ou, X. Li, B. Liu, Y. Huang, S.T. Ho. Optics lett., **35** (10), 1721 (2010).
[5] W.W. Wong, C. Jagadish, H.H. Tan. IEEE J. Quant. Electron., **58** (4), 1 (2022).
[6] X.M. Lv, Y.Z. Huang, Y.D. Yang, H. Long, L.X. Zou, Q.F. Yao, X. Jin, J.L. Xiao, Y. Du. Opt. Express, **21** (13), 16069 (2013).
[7] S.J. Choi, K. Djordjev, S.J. Choi, P.D. Dapkus. IEEE Photon. Technol. Lett., **15** (10), 1330 (2003).
[8] W. Xie, T. Stöferle, G. Raino, T. Aubert, S. Bisschop, Y. Zhu, R.F. Mahrt, P. Geiregat, E. Brainis, Z. Hens, D.V. Thourhout. Advanced Mater., **29** (16), 1604866 (2017).
[9] X. Xu, T. Maruizumi, Y. Shiraki. Opt. Express, **22** (4), 3902 (2014).
[10] L.X. Zou, X.M. Lv, Y.Z. Huang, H. Long, Q.F. Yao, Y. Du. Optics and Photonics J., **3** (2), 66 (2013).
[11] N.V. Kryzhanovskaya, K.A. Ivanov, N.A. Fominykh, S.D. Komarov, I.S. Makhov, E.I. Moiseev, J.A. Guseva, M.M. Kulagina, S.A. Mintairov, N.A. Kalyuzhnyy, A.I. Lihachev, R.A. Khabibullin, R.R. Galiev, A.Yu. Pavlov, K.N. Tomosh, M.V. Maximov, A.E. Zhukov. J. Appl. Phys., **134** (10), 103101 (2023).
[12] D. Inoue, Y. Wan, D. Jung, J. Norman, C. Shang, N. Nishiyama, S. Arai, A.C. Gossard, J.E. Bowers. Appl. Phys. Lett., **113** (9), 093506 (2018).
[13] N.V. Kryzhanovskaya, S.A. Blokhin, I.S. Makhov, E.I. Moiseev, A.M. Nadtochiy, N.A. Fominykh, S.A. Mintairov, N A. Kalyuzhny, Yu.A. Guseva, M.M. Kulagina, F.I. Zubov, E.S. Kolodezny, M.V. Maksimov, A.E. Zhukov. FTP, **57** (3), 202(2023). (in Russian).
[14] N.V. Kryzhanovskaya, E.I. Moiseev, A.M. Nadtochiy, A.A. Kharchenko, M.M. Kulagina, S.A. Mintairov, N.A. Kalyuzhny, M.V. Maksimov, A.E. Zhukov. Pis'ma ZhTF, **46** (13), 7 (2020). (in Russian).
[15] S.A. Mintairov, N.A. Kalyuzhnyy, V.M. Lantratov, M.V. Maximov, A.M. Nadtochiy, S. Rouvimov, A.E. Zhukov. Nanotechnology, **26** (38), 385202 (2015).
[16] M.K. Chin, S.T. Ho. J. Lightwave Technol., **16** (8), 1433 (1998).
[17] F. Zubov, M. Maximov, E. Moiseev, A. Vorobyev, A. Mozharov, Yu. Berdnikov, N. Kaluzhnyy, S. Mintairov, M. Kulagina, N. Kryzhanovskaya, A. Zhukov. Optics Lett., **46** (16), 3853 (2021).
[18] J. Huang, Y. Wan, D. Jung, J. Norman, C. Shang, Q. Li, K.M. Lau, A.C. Gossard, J.E. Bowers, B. Chen. ACS Photonics, **6** (5), 1100 (2019).

Translated by A.Akhtyamov